A Unifying Modelling Formalism for the Integration of Stoichiometric and Kinetic Models

Jorge Júlvez [a,⋆], Stephen G Oliver [b,c]

[a] *Department of Computer Science and Systems Engineering, University of Zaragoza, Zaragoza, Spain*

[b] *Cambridge Systems Biology Centre, University of Cambridge, Cambridge, UK*

[c] *Department of Biochemistry, University of Cambridge, Cambridge, UK*

Abstract

Current research on systems and synthetic biology relies heavily on mathematical models of the systems under study. The usefulness of such models depends on the quantity and quality of biological data, and on the availability of appropriate modelling formalisms that can gather and accommodate such data so that they can be exploited properly. Given our incomplete knowledge of biological systems and the fact that they consist of many subsystems, biological data are usually uncertain and heterogenous. These facts hinder the use of mathematical models and computational methods. In the scope of dynamic biological systems, e.g. metabolic networks, this difficulty can be overcome by the novel modelling formalism of Flexible Nets (FNs). We show that an FN can combine, in a natural way, a stoichiometric model and a kinetic model. Moreover, the resulting net admits nonlinear dynamics and can be analysed in both transient and steady states.

Key words: Systems biology; Modelling formalisms; Stoichiometric models; Kinetic models; Flexible Nets

1 Background

Mathematical models play a crucial role in the study and understanding of biological systems. They may be used to efficiently predict system behaviour, to reason about system properties, to elaborate (or exclude) hypotheses, to speed up the design of experiments and, as an unambiguous language, to exchange data among practitioners. As an increasing amount of biological data is available, mathematical models must be able to accommodate such data and the computational methods associated with them must be robust enough to account for any possible missing information. Given that biological systems are composed of many connected subsystems, existing biological data are heterogeneous and refer to the particular subsystem(s) being studied. This often leads to the adoption of several modelling formalisms [1] for the study of a single system, each of these formalisms being used to model a particular subsystem.

Some of the most popular modelling formalisms for biological systems are: *Boolean networks* [2,3], which are networks of Boolean variables that are mainly used to model gene regulatory networks [2] and signalling pathways [4]; *Bayesian networks* [5,6], which are a particular type of probabilistic graph that can model gene regulation [7] and signalling networks [8]; *Petri nets* [9], which are bipartite graphs that have been mainly used to model metabolic and gene regulatory networks [10,11]; *constraint-based models* [12,13] are popular for their ease to include flux bounds on the reactions of large metabolic networks, e.g. on the exchange reactions that model the feed of nutrients; *differential equations* are a classical and powerful formalism to model the dynamics of systems whose parameters are known with precision [14,15]. A comprehensive review of modelling formalism in systems biology can be found in [1].

The use of several of these modelling formalisms to model the different parts of a system hampers the analysis tasks as they are usually difficult to connect and they might not share computational methods. Moreover, the resulting model tends to provide a less clear view of the overall system. Thus, there is a need for general modelling formalisms that can integrate, in a natural way, the available biological data of subsystems in a unified model. We propose here Flexible Nets (FNs) as an appropriate modelling formalism that subsumes the modelling capabilities of both constraint-based models and differential equations. As a proof of concept, it will be shown how the stoichiometric model of a metabolic net-

⋆ Corresponding author. E-mail: julvez@unizar.es

work, modelled by a constraint-based model, and the kinetics of a bioreactor, modelled by differential equations, are combined in a single model by FNs.

FNs were defined in [16] and are inspired by Petri nets [9,17]. However, in contrast to Petri nets which are bipartite graphs, an FN consists of two connected subnets, an *event net* and an *intensity net*, each of which is a tripartite graph. The three vertices of these nets are *places*, *transitions*, and *handlers*. While the event net accounts for the stoichiometry of the system, the intensity net models the kinetics of the reactions. Handlers represent an intermediate layer between places (which model metabolites) and transitions (which model reactions), and capture the way in which the occurrence of a reaction modifies the concentration of metabolites (event handler), and the way in which the concentration of metabolites modulates the reaction rates (intensity handler). Uncertain parameters can be incorporated easily in an FN by associating inequalities to handlers. Among other possibilities, handlers facilitate the modelling of partially observable systems, constrained control actions and resource allocation [18]. Moreover, it will be shown that the association of several sets of inequalities with intensity handlers allows the modelling of reactions with nonlinear rates. This leads to a powerful modelling formalism able to handle uncertain parameters and nonlinear dynamics.

In addition to their modelling features, FNs are equipped with computational methods to analyse both the transient and steady states of the modelled system. In order to account for the uncertainties in the FN, sets of mathematical constraints that are necessarily satisfied by the state variables are derived. These sets of constraints, together with an objective function, are the basis of the computational methods to bound all the potential behaviours of the system.

2 Methodology

This section introduces the modelling formalism of Flexible Nets (FNs) and presents its main features through examples. The focus is on systems that can be described as networks of reactions, e.g. metabolic networks, signalling networks, gene regulatory networks, etc. It will be shown that FNs are particularly useful to model systems with partially unknown data. More precisely, one of the main strengths of FNs is that they are able to integrate seamlessly in a single model all the available data about the system as well as to accommodate the existing parameter uncertainties.

We will first describe how the stoichiometry of reactions can be modelled, and then how the reaction kinetics can be incorporated into the model.

2.1 Modelling the stoichiometry

FNs is a modelling formalism that provides an intuitive graphical representation of the modelled system. The system is represented graphically as a net in which the *vertices* are connected by *edges*. There are three different types of vertices: *places* (which are represented as circles), *transitions* (which are represented as rectangles) and *handlers* (which are represented as dots). The edges can be directed and undirected. For simplicity, directed edges are referred as *arcs*, and undirected edges as *edges*.

In an FN, places model the chemical species (or metabolites) of the system, and transitions model the rates of the reactions of the system. FNs account for the following relationships between places, i.e. chemical species, and transitions, i.e. reaction rates:

(1) The occurrence of a reaction modifies the concentration (or copy number) of the chemical species.
(2) The concentration of the chemical species determines the rate of reactions.

These two relationships are modelled by handlers: *event handlers* model the stoichiometry, i.e. the concentration changes due to the occurrence of reactions; *intensity handlers* model the way in which concentrations determine the rate of reactions.

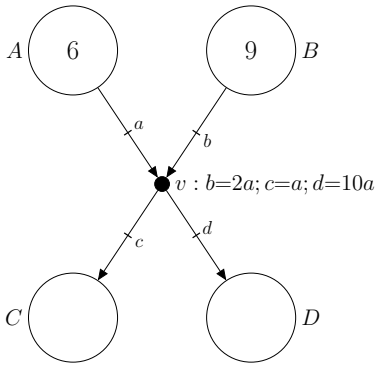

Fig. 1. FN modelling the stoichiometry of the reaction $R : A + 2B \to C + 10D$.

Consider the reaction $R : A + 2B \to C + 10D$ which has two reactants, A and B, two products C and D, and is not reversible. Reaction R is modelled by the FN in Fig. 1 which has 4 places, 4 arcs, and one event handler. Each place is associated with a chemical species and the reaction itself is modelled by the event handler v. An arc from a place to v means that the place is a reactant, and an arc from v to a place means that the place is a product. Each arc has a label that is used in a set of equations associated with the handler to determine the stoichiometry of the reaction. For the sake of generality, we will not refer to particular concentration or copy number units here (e.g. mmol, molecules) and will just use the term "units" to refer to amounts of chemical species. In this particular case, the equations $b = 2a$; $c = a$; $d = 10a$ mean that when R occurs two units of B are consumed for each unit of A that is consumed (i.e. B decreases twice as much as A), one unit of C is produced for each unit of A that is consumed, and 10 units of D are produced for each unit of A that is consumed.

The concentration of a chemical species can be repre-

sented by a number located in the place associated with the species. In the Flexible (and Petri) nets jargon such a number is called marking and it is denoted by m, i.e. $m[A] = 6$ and $m[B] = 9$ in Fig. 1 mean that the concentrations of A and B are 6 and 9 units, respectively. Initial concentrations are denoted by m_0. Uncertain concentrations can be modelled by means of inequalities assciated with the FN. For example, the inequalities $5 \leq m_0[A] \leq 8$ and $m_0[B] = 2m_0[A]$ would model that the initial concentration of A is unknown but lies in the interval $[5, 8]$ and that the initial concentration of B is twice as much as the concentration of A.

Uncertain stoichiometric weights can be easily modelled by associating a set of inequalities (instead of equalities) to event handlers. For instance, the association of $b = 2a; c = a; 9a \leq d \leq 11a$ with v in Fig. 1 models a reaction with uncertain stoichiometry, $R : A + 2B \rightarrow C + nD$, where n is uncertain, but known to be in the interval $[9, 11]$, i.e. for each unit of A that is consumed between 9 and 11 units of D are produced (the particular number of units produced is unknown). This feature of FNs is particularly useful to model the assembly or degradation of large macromolecular complexes with uncertain numbers of components.

In the FNs presented so far, the reaction rates (or fluxes) are not specified and could be any nonnegative value (including 0 and ∞). Stoichiometric models of metabolic networks sometimes include numerical information about the fluxes of their reactions. This information, which usually refers to lower and upper flux bounds, i.e. the minimum and maximum values of the flux of transitions, can be incorporated into an FN by means of a transition connected to the handlers modelling the reactions.

In an FN, each transition t is assigned a default intensity (or speed), which is denoted $\lambda_0[t]$. This intensity can be used to produce reaction rates on the event handlers connected to t. For instance, assume that in the FN in Fig. 2 the default intensity of R is $\lambda_0[R] = 2$ and the equations associated with v are $v : x{=}a; b{=}2a; c{=}a; d{=}10a$. This implies that the flux of the reaction is equal to 2 which is the value assigned to the label x of the edge connecting R and v (2 is also the rate at which A is consumed).

Similarly to the initial marking of places, default intensities can be bounded by a set of linear inequalities if their precise value is unknown. Let us associate the inequalities $1 \leq \lambda_0[R] \leq 4$, then the default intensity of R can be any value in the interval $[1, 4]$, i.e. the lower flux bound of R is 1 and its upper flux bound is 4.

A reaction in a stoichiometric model is reversible if its net flux can be positive or negative, i.e. reactants can be produced and consumed. This is expressed with a negative lower bound and a positive upper bound. Given that default intensities cannot be negative, reversible reactions are modelled in FNs by two non-reversible reactions, a forward reaction and a backward reaction, such that the forward reaction models consumption of reactants and the backward reaction models production of

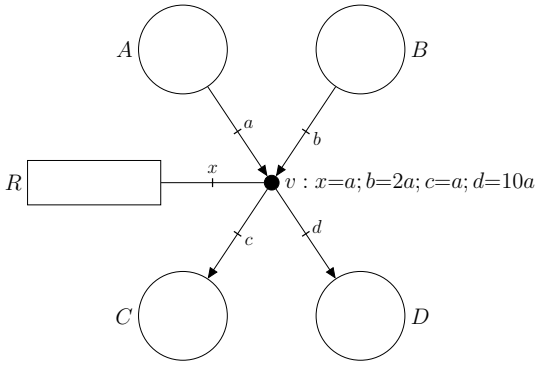

Fig. 2. Reaction $R : A + 2B \rightarrow C + 10D$ with flux bounds modelled by $\lambda_0[R]$, e.g. $1 \leq \lambda_0[R] \leq 4$.

reactants. The lower bounds of both reactions are set to 0, the upper bound of the forward reaction is equal to the upper bound of the reversible reaction, and the upper bound of the backward reaction is equal to minus the lower bound of the reversible reaction.

Consider the reversible reaction $R : A + 2B \leftrightarrow C + 10D$ with flux bounds $[-2, 8]$. The FN in Fig. 3 models such a reversible reaction by setting $0{\leq}\lambda_0[R_f]{\leq}8$, $0{\leq}\lambda_0[R_b]{\leq}2$ and by associating the same set of equalities with both handlers v_f and v_b, i.e. $v_f{:}x{=}a; b{=}2a; c{=}a; d{=}10a$ $v_b{:}x{=}a; b{=}2a; c{=}a; d{=}10a$.

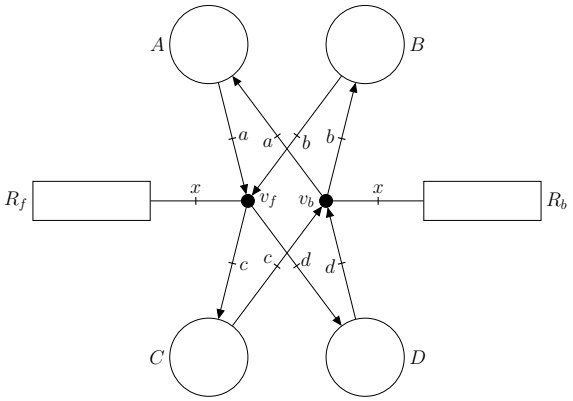

Fig. 3. FN modelling the reversible reaction $R : A + 2B \leftrightarrow C + 10D$.

2.2 Modelling the kinetics

In the modelling examples presented above, the rate of the reactions is independent of the metabolite concentrations. This is usually the case for stoichiometric models in which the stoichiometry of reactions together with some steady state flux bounds are specified. However, more detailed kinetic information might be available for some organisms/systems that should be incorporated into the model in order to increase its accuracy and modelling power. Such kinetic information can be accommodated in FNs by means of *intensity handlers*.

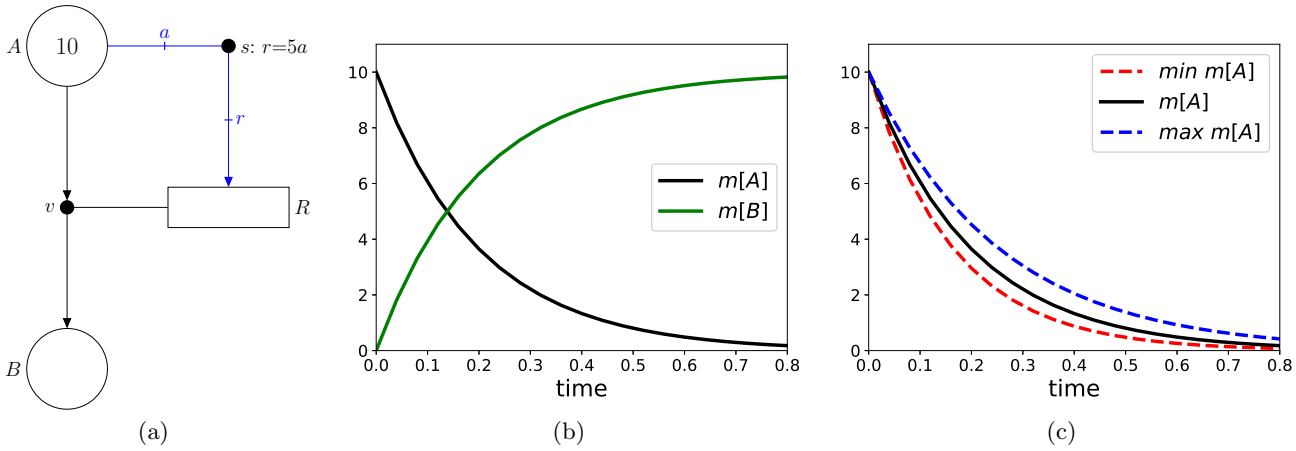

Fig. 4. (a) FN modelling a reaction $R : A \to B$ with rate equal to five times the concentration of A; (b) Trajectory of the concentrations of places A and B; (c) Maximum and minimum trajectories of the concentration of place A when $4a \leq r \leq 6a$ is associated with s.

Consider the reaction $R : A \to B$ with rate equal to five times the concentration of A. Such a reaction is modelled by the FN in Fig. 4(a). As in the previous section, the stoichiometry of the reaction is modelled by the places A and B, by the event handler v, by the arcs (A, v) and (v, B), and by the edge $\{R, v\}$. These elements compose the so-called *event net*. Note that the labels of (A, v), (v, B), and $\{R, v\}$ have been omitted for the sake of clarity. When the labels are omitted, it is assumed that all the labels are made equal by the equations associated with the handler (v in this case), e.g. if the name of the labels of (A, v), (v, B) and $\{R, v\}$ were a, b and x respectively, then the equations associated with v are $a = b$ and $a = x$ (i.e. if the reaction occurs once, then one unit of A is consumed and one unit of B is produced).

The rate of the reaction is equal to the intensity of the transition R, which is denoted $\lambda[R]$, associated with it. If no arc is connected to the transition, then its intensity is equal to its default intensity, i.e. $\lambda[R] = \lambda_0[R]$. The intensity of a transition can be increased by incoming arcs that originate in an intensity handler (conversely, it can be decreased by outgoing arcs to an intensity handler). The FN in Fig. 4(a) has one intensity handler s connected to place A and transition R. The edge $\{A, s\}$ means that the concentration in A is used to produce intensity, and the arc (s, R) together with the equation $r = 5a$ of s means that the intensity produced in R is five times the concentration of A. The places, transitions and elements in blue in Fig. 4(a) compose the so-called *intensity net* that determines the rates of reactions. Although, event and intensity handlers can be distinguished graphically by their arcs and edges (event handlers are connected to places by arcs and to transitions by edges; intensity handlers are connected to places by edges and to transitions by arcs), in order to make the presentation clearer, arcs and edges connected to event handlers will be depicted in black, and arcs and edges connected to intensity handlers will be depicted in blue.

Figure 4(b) shows the time trajectory of the concentration of places A and B assuming that the initial concentrations of A and B are 10 and 0, respectively. Similarly to uncertain stoichoimetric weights modelled by the event net, inequalities can be associated with intensity handlers in order to model uncertain reaction rates. Assume that the reaction rate of R is uncertain but known to be in the interval $[4a, 6a]$ where a is the concentration of A. This can be modelled by associating the inequality $4a \leq r \leq 6a$ with s. This leads to a spectrum of potential time evolutions of the system. Although such a system becomes nondeterministic, its behaviour can still be analysed by computing bounds of the potential time trajectories. The dotted trajectory in blue(red) in Fig. 4(c) corresponds to the upper bound or maximum(lower bound or minimum) of all the potential trajectories that satisfy the constraint that the reaction rate is in the interval $[4a, 6a]$ (the black line is the deterministic trajectory when the rate is $5a$). Thus, FNs make it possible to constrain the potential trajectories of a system with uncertain reaction rates.

An appealing modelling feature of FNs is the ease with which they model complex regulatory networks in which two or more enzymes must act at the same time to modulate the rates of reactions. The FN in Fig. 5 models three reactions $R_1 : A \to B$, $R_2 : C \to D$ and $R_3 : E \to F$ that are regulated by enzymes X, Y and Z. Notice that while A, B, C, D, E and F have incoming and outgoing arcs, i.e. they are consumed and produced, X, Y and Z are only connected by edges to intensity handlers, i.e. their concentrations are always constant and are used to produce intensities. Given that place X has two edges, its concentration can be used either to produce intensity in R_1 through s_1 or in R_2 through s_2. Thus, the concentration of X is divided into two parts, one of them produces intensity in R_1 and the other in R_2. Similarly, Y can produce intensity in R_1 and R_3, and Z can increase the intensity of R_2 and decrease the intensity of R_3 (the decrease is modelled by the arc (R_3, s_5)).

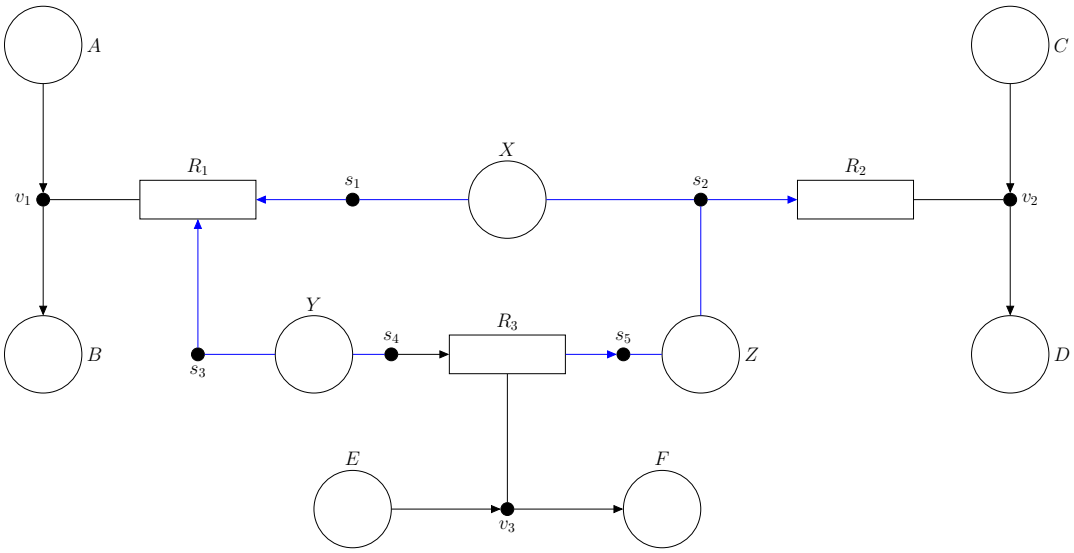

Fig. 5. FN modelling three reactions catalysed by enzymes.

More precisely, the rate of R_1 is equal to the concentration of X applied on s_1 plus the concentration of Y applied on s_3 (thus the rate is the sum of the applied concentrations). Reaction R_2 has only one incoming arc with intensity equal to the concentration of X applied on s_2 and equal to the concentration of Z applied on s_2. This implies that X and Z need to act at the same time, for instance by forming a compound, in equal amounts, e.g. α in order to produce an intensity α in R_2. Finally, the rate of R_3 is equal to the concentration of Y applied on s_4 minus the concentration of Z applied on s_5 (in this case, Y can be seen as an enhancer and Z as a repressor). Notice that the resulting FN provides an intuitive graphical representation in which the regulation, i.e. the intensity net composed of X, Y and Z, is clearly separated from the production and consumption part of the system, i.e. the event net composed of A, B, C, D, E and F.

In the FNs presented so far the rate of reactions is either constant or proportional to the concentration of metabolites, i.e. there is a linear relationship between rates and concentrations. This kind of relationship is not enough to model many of the complex and nonlinear reaction rates in biological systems. In order to account for such nonlinearities, FNs offer the possibility of analysing piecewise linear functions with intensity handlers.

The FN in Fig. 6 models three reactions:

- $R_1 : \emptyset \to A$
- $R_2 : A \to \emptyset$
- $R_3 : \emptyset \to B$

such that the rate of R_1 is constant and equal to 2 (this is modelled by $\lambda_0[R_1] = 2$), the rate of R_2 is equal to the concentration of A (this is modelled by the equation $r = a$ in s_1) and the rate of R_3 depends piecewise linearly on A. More precisely, the equations "$t = 0$ if $a < 1$" and "$t = a$ otherwise" in s_1 imply that the rate of R_3 is 0 if the concentration of A is less than or equal to 1.0, and equal to the concentration of A if it is greater than 1.0, i.e. this FN models the activation of the reaction R_3 when the concentration of A is sufficiently high.

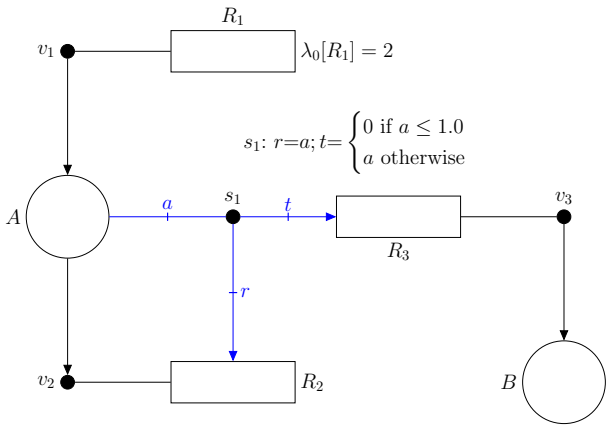

Fig. 6. Reaction R_3 is activated when the concentration of A is greater than 1.0.

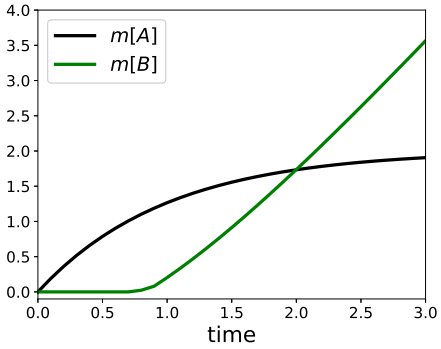

Fig. 7. Trajectories of the concentrations of places A and B of the FN in Fig. 6.

Figure 7 shows the time trajectories of the concentrations of A and B assuming that their initial value is 0. While the concentration of A tends asymptotically to 2.0, the rate of R_3, and hence the concentration of B, is constant and equal to 0 until A crosses the threshold of 1.0. From that time instant on, the rate of R_3 is equal to the concentration of A, and B increases.

The association of piecewise linear functions with intensity handlers can be used to approximate genuinely nonlinear reaction rates. The FN in Fig. 8(a) shows a reaction $R : A \to \emptyset$ with a rate that follows a particular Hill equation $\theta = \frac{[L]^n}{K_d+[L]^n}$ with $K_d = 1$ and $n = 3$; see the equation associated with the intensity handler s. The analysis methods of FNs rely on the solution of the mixed-integer linear programming problems that are derived from the models. Such a derivation is only possible if the equations associated with the intensity handlers are piecewise linear. Thus, the Hill equation, which is shown in Fig. 8(b), cannot be handled directly by the analysis methods of FNs. In order to analyse the FN in Fig. 8(a), the Hill equation must be approximated by a piecewise linear function. A possible piecewise linear approximation of such an equation is shown in Fig. 8(c). The computed approximation partitions the state space of the concentration of A in 7 regions and associates a linear function with each region. The equations that approximate the Hill function, and that are associated with s, are:

$$s\text{: } r = \begin{cases} 0.039a & \text{if } a < 0.2 \\ -0.051 + 0.270a & \text{if } 0.2 \leq a < 0.4125 \\ -0.194 + 0.617a & \text{if } 0.4125 \leq a < 0.625 \\ -0.310 + 0.810a & \text{if } 0.625 \leq a < 1.05 \\ -0.009 + 0.530a & \text{if } 1.05 \leq a < 1.475 \\ +0.388 + 0.258a & \text{if } 1.475 \leq a < 1.9 \\ +0.783 + 0.058a & \text{otherwise} \end{cases}$$

Notice that the density of regions is higher in those intervals in which the rate has more variability. The resulting time trajectory of the concentration of A together with the regions it visits are shown in Figure 8(d). It should be noticed that the partition of the state space in regions can be performed automatically (e.g. with the *fnyzer* Python package [19]) in order to minimize the error of the piecewise linear approximation to the nonlinear function.

2.3 Model integration

FNs are particularly useful for integrating the known information about the kinetics of the reactions of a system into a single net model. This information can be either none (i.e. nothing is known about the reaction rate), or partially known (i.e. there is some uncertainty in the parameters that define the rate) or completely known (i.e. there is a well-known equation with accurate parameters defining the reaction rate). An example of such integration in a single model is shown in Fig. 9 which models the system of reactions listed in Table 1.

Reaction	Modelled by
$R_1 : \emptyset \to A$	v_1
$R_2 : \emptyset \to B$	v_2
$R_3 : A \to C$	v_3
$R_4 : 2A + B \to D$	v_4
$R_5 : C \to \emptyset$	v_5
$R_6 : D \to \emptyset$	v_6 and s_1

Table 1
Reactions modelled by the FN in Fig. 9.

The following information for the reaction rates is assumed:

- The rates of R_3, R_4 and R_5 are completely unknown. Hence, these reactions are modelled just by the event handlers v_3, v_4 and v_5 which are connected through arcs to the places that model reactants and products. Event handlers v_3 and v_5 have no *explicit* equations associated with them (and their arcs have no labels), thus, this implies that all the stoichiometric weights of reactions R_3 and R_4 are equal to 1. On the other hand, the equations $a = 2b$ and $d = b$ associated with v_4 imply that two units of A are consumed per each unit of B, and that one unit of D is produced per each unit of B that is consumed.
- The rate of R_2 is uncertain and known to be in the interval $[2, 4]$. This is modelled by the inequalities $2 \leq \lambda_0[t_2] \leq 4$ associated with transition t_2.
- The rates of R_1 and R_6 are completely known. The rate of R_1 is equal to 6 which is modelled by the equation $\lambda_0[t_1] = 6$ associated with t_1. The rate of R_6 is equal to the concentration (or marking) of D which is modelled by the intensity handler s_1 and the edge and arc connecting it to D and t_3.

Given that the described system of reactions contains uncertain dynamics, its analysis should consider all the potential time evolutions that are consistent with the known information. The computational methods in [16] and [20] develop a set of mathematical inequalities (or constraints) that the state (i.e. concentrations, rates, etc.) of the FN must satisfy over time and in the steady state, respectively. Such constraints can be interpreted as necessary reachability conditions and account for all the potential states that the FN can reach. These sets of constraints can be combined with an objective function in order to study the behaviour of the system by solving the associated programming problems. That is, the computational methods developed for FNs can analyse nondeterministic models.

As an example of the analysis capabilities in FNs, let us compute concentration bounds of D in Fig. 9 in the long run, i.e. in the steady state. A steady state lower bound of D can be obtained by associating the objective function $min\ \overline{m}[D]$, where $\overline{m}[D]$ denotes the average steady state concentration of D, with the constraints described in [20]. The obtained lower bound is 2.0; with

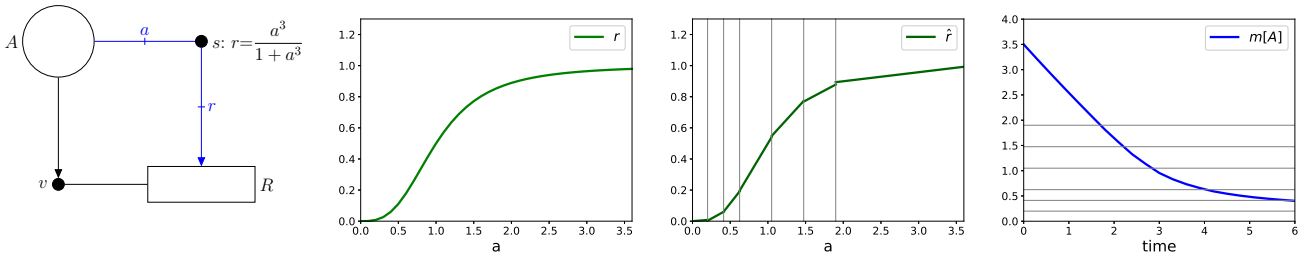

(a) (b) (c) (d)

Fig. 8. (a) FN modelling a reaction R with rate following a Hill equation; (b) Hill equation; (c) Piecewise linear approximation; (d) Trajectory of the concentration of A.

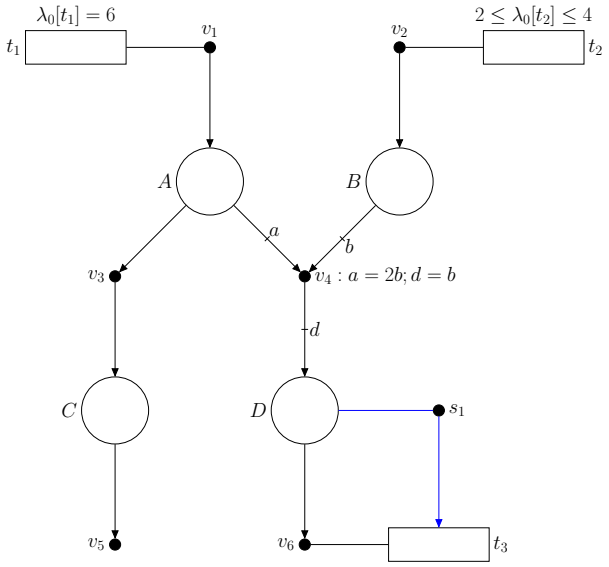

Fig. 9. Integration of reactions with and without dynamic information.

such a concentration, the rate of R_6 is 2.0, i.e. in the steady state, the flux coming into (production rate) D and going out of (consumption rate) D is 2.0. Given that v_4 establishes that B is consumed at the same rate at which D is produced, the rate of R_4 is necessarily 2.0 and therefore the rate of R_2 is also 2.0 (which is in the range $[2, 4]$ established by $2 \leq \lambda_0[t_2] \leq 4$). A rate 2.0 of R_4 implies that R_4 consumes A at a rate 4.0 and hence, given that A is produced by R_1 at rate 6.0, it must be consumed by R_3 at rate 2.0. In the steady state, the production and consumption rate of C is also 2.0.

The solution of the programming problem associated with the FN and the objective function set does not only provide a lower bound of D, but also the state of the FN that achieves that value, i.e. all the mentioned values, which are reported in Table 2 (row "Lower bound"), are given by the solution of the programming problem.

Similarly, an upper bound of D can be computed by considering the objective function $max\ \overline{m}[D]$. For such a function, the obtained upper bound is 3.0, the rate of R_6, the flux through B, and the rate of R_2 is also 3.0. This implies that A is consumed by R_4 at the same rate at which it is produced by R_1, and hence the rate of R_3 and the flux through C is also 0.0. The obtained reaction rates are reported in Table 2 (row "Upper bound").

3 Results

The ability of FNs to integrate stoichiometric and kinetic models in a single net is exploited in this section to model and analyse a continuous cell culture that takes place in a bioreactor [21]. The considered stoichiometric model is a simplified metabolic network of mammalian HeLa cells [22], and the kinetic model is given by the differential equations that determine the evolution of the main bioreactor variables [23]. Figure 10 sketches the layout of the system which is composed of three main parts: a *reservoir* that contains a sterile growth medium that is fed into the bioreactor; a *bioreactor* (or *tank*) which is assumed to be well-mixed and that contains the cell culture; and an *effluent* that discharges the excess volume of the bioreactor.

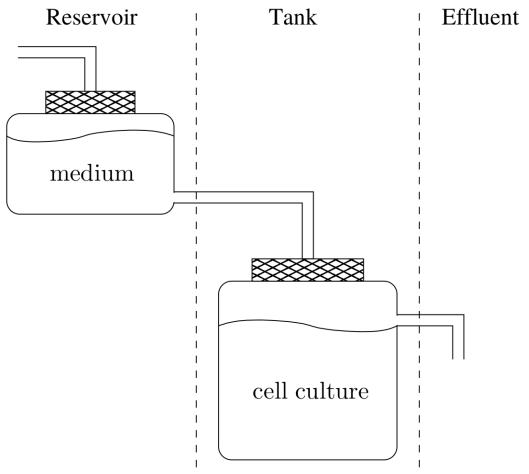

Fig. 10. Sketch of a continuous cell culture in a bioreactor.

The overall system was introduced in [23] where a method similar to Dynamic Flux Balance Analysis (DFBA) [24] was used to determine the potential steady states of the system. We show here that the differential equations associated with the bioreactor and the constraint-based model of the metabolic network of the

	Objective function	$m[D]$	R_1	R_2	R_3	R_4	R_5	R_6
Lower bound	$min\ m[D]$	2.0	6.0	2.0	2.0	2.0	2.0	2.0
Upper bound	$max\ m[D]$	3.0	6.0	3.0	0.0	3.0	0.0	3.0

Table 2
Steady state lower and upper bounds of the concentration of D ($m[D]$) and reaction rates of the FN in Fig. 9.

cells in the culture can be accommodated in a single FN which represents graphically the system structure and that offers appealing analysis possibilities.

3.1 System description

We will first describe the bioreactor variables (these can be seen as macroscopic variables) and then the metabolic network of the cells.

Bioreactor: The differential equation that defines the evolution of the cell density in the tank is:

$$\frac{\mathrm{d}X}{\mathrm{d}t} = (\mu - \phi D)X \tag{1}$$

where X is the cell density in the tank ($gDW\ L^{-1}$), μ is the effective cell growth rate (h^{-1}), ϕ is a unitless bleeding coefficient accounting for the fraction of cells that escape from the tank through a cell-retention device [25] and D is the dilution rate (h^{-1}). It should be stressed that the employment of the cell retention device means that the relationship between cell density and dilution rate will not follow classical chemostat kinetics [26].

The evolution of the concentration of metabolites in the culture is given by:

$$\frac{\mathrm{d}s_i}{\mathrm{d}t} = (c_i - s_i)D - u_i X \tag{2}$$

where c_i is the concentration of metabolite i in the medium (mM), s_i is the concentration of metabolite i in the culture (mM) and u_i is the specific uptake rate of metabolite i ($mmol\ gDW^{-1}\ h^{-1}$). Notice that if $u_i > 0$ the metabolite is consumed by the cell and if $u_i < 0$ the metabolite is excreted from the cell.

Metabolic network: While the values of D, s_i and ϕ can be controlled when setting up the system, the values of μ, u_i and in turn s_i will depend on the particular cell line being cultured and, in particular, on its metabolic network. The focus here is on a reduced metabolic network of HeLa cells which is modelled by the FN in Fig. 11 and that exemplifies some of the main features of FNs.

The places in the FN model the four metabolites that are taken into account: S is the primary nutrient, P is an intermediate, E is the energetic currency, and W is a waste product. The consumption of S from the medium by the cell is modelled by the arc going from the event handler v_u to the place S. It should be noted that the direction of the arc (v_u, S) imposes consumption of the metabolite, i.e. the consumption rate will be $u_s \geq 0$, if a metabolite can be both consumed and excreted, then a reversible reaction should be used; see Fig. 3. The nutrient S is processed into P, see arcs (S, v_s) and (v_s, P).

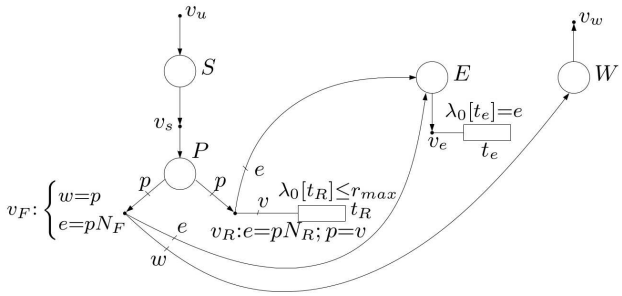

Fig. 11. FN modelling a simplified metabolic network of a HeLa cell.

Reaction	Modelled by
$R_u:\ \emptyset \to S$	v_u
$R_s:\ S \to P$	v_s
$R_F:\ P \to N_F E + W$	v_F
$R_R:\ P \to N_R E$	v_R
$R_e:\ E \to \emptyset$	v_e
$R_w:\ W \to \emptyset$	v_w

Table 3
Reactions of the metabolic network in Fig. 11.

The intermediate P can undergo either fermentation, modelled by v_F, or respiration, modelled by v_R. These alternative paths are modelled by the arcs (P, v_F) and (P, v_R) respectively. On the one hand, fermentation produces N_F units of energy , see arc (v_F, E), and one unit of waste product, see arc (v_F, W). On the other hand, respiration produces N_R units of energy, see arc (v_R, E). The values of N_F and N_R [27] are reported in Table 5.

The energy consumption of the cell E is modelled by the arc (E, v_e), and the excretion of the waste product W from the cell is modelled by the arc (W, v_w). This way, the list of the reactions of the described metabolic network are reported in Table 3.

The information provided so far about the metabolic network refers exclusively to its stoichiometry, i.e. only *arcs* have been discussed and no kinetic parameter has been introduced. Thus, under the current description, the reactions can proceed at any rate. Let us constrain the rate of reactions R_e and R_R. It will be assumed that a

constant energetic demand is required by the cell [28,29], this is modelled by transition t_e, by the *edge* $\{t_e, v_e\}$, and by the default intensity $\lambda_0[t_e]{=}e$ associated with t_e. On the other hand, reaction R_R has an important enzymatic cost [30] and hence its rate must be bounded. This can be achieved by associating the inequality $\lambda_0[t_R]{\leq}r_{max}$ with reaction t_R which is connected through an arc to event handler v_R.

It should be noted that, although the rates (or fluxes) of R_e and R_R have been constrained, the FN that models the metabolic network is exclusively an event net, i.e. there are no intensity handlers and hence the reaction rates do not depend on the concentrations of the metabolites. This is usually the case for most genome-scale metabolic networks in the literature.

3.2 Model integration

The integration of the discussed metabolic network with the equations (1) and (2) that describe the dynamics of the bioreactor variables requires an interface that relates the variables of both models. Let us first describe how equations (1) and (2) can be modelled in terms of FNs. In order to do so, we will consider the three parts of the bioreactor - *reservoir*, *tank*, and *effluent* - separately; see Fig. 10. The resulting FN that integrates the bioreactor variables and the metabolic network is shown in Fig. 12.

The model for the *reservoir* (see compartment *reservoir* in Fig. 12) just needs to account for a flux of nutrient S going into the tank. Such a flux is equal to the dilution rate D times the concentration c of the nutrient S in the medium. This is modelled by the default intensity $\lambda_0[t_{sin}]{=}Dc$ associated with transition t_{sin} and the event handler v_{sin} that feeds the place S_{tank}.

The variables that describe the state of the *tank* are the nutrient concentration, the cell density, and the waste product concentration; these are modelled by places S_{tank}, X and W_{tank} respectively. While the dynamics of X is ruled by (1), the dynamics of both S_{tank} and W_{tank} are determined by (2).

With respect to S, equation (2) establishes that S has one input flux equal to Dc from the reservoir (previously discussed) and two output fluxes: 1) a flux equal to uX, where u is the consumption rate of the cells, that goes into the cells, i.e. is consumed by the cells, and; 2) a flux equal to Ds, where D is the dilution rate and s is the concentration of the nutrient S in the tank, which leaves the tank as effluent without being consumed by the cells. These two fluxes are modelled by the arcs (S_{tank}, v_{ut}) and (S_{tank}, v_{sout}). The fact that the flux leaving the tank is proportional to the concentration of S is modelled by the intensity handler s_{sout} which is associated with the equation $s_{sout}{:}r{=}Ds$. The flux going into biomass must be linked to the fluxes of the metabolic network and is discussed below.

Given that there is no waste product in the medium, equation (2) just establishes one input flux and one output flux for the waste product W in the tank. The output flux is similar to that of S and it is proportional to the concentration of W in the tank. This is modelled by the intensity handler s_{wout} and the equation $r{=}Dw$ associated with it.

With respect to the cell density X, equation (1) states that it has one input flux and one output flux. The output flux follows a similar pattern to those of S and W and is equal to ϕDx.

The interface (or link) between the tank variables and the metabolic network is achieved by means of the intesity handlers s_u, s_r and s_w that connect the compartments $Tank$ and $Cell$ in Fig. 12. These handlers relate the fluxes of the macroscopic variables with the exchange fluxes of the cells as follows: each macroscopic flux is equal to X times the exchange flux of the cell, where X is the cell density in the tank. This is modelled by the equations $u_t = uX$, $t_t = rX$ and $w_t = vX$ associated with the handlers. In addition to $u_t = uX$, the equation $u{\leq}V$ associated with s_u bounds the maximum uptake rate of the nutrient by the cell.

The input flux of X deserves special attention. According to (1), its input flux is μX where μ is the effective cell growth rate. The value of μ is obtained by $\mu = z - \tau w$ where z is proportional to the flux of E consumed for biomass production (see arc (E, v_x)). Thus, it is assumed that E is a direct precursor of biomass and $e = yz$ where e is the flux of E used for biomass production and y is constant (see equation associated with v_x). On the other hand, the term τw, where w is the concentration of W in the tank and τ is a constant, models the toxicity of the waste product and quantifies the amount in which it inhibits growth. This inhibition is modelled by the arc (t_{xt}, s_{wout}) which subtracts an intensity (or growth rate) amount of τwX, see equation associated with s_{wout}, to transition t_{xt}.

It should be noted that the equations associated with s_u, s_r, s_w and s_{wout} are not linear , e.g. the equation associated with s_u contains the multiplication of two variables, the cell density, X, and the intensity of arc (s_u, t_u), and must be approximated as nonlinear functions in a similar way to the Hill function in Fig. 8. This is achieved by partitioning the interval $[0.0, 3.0]$, where the cell density X lies, into 250 regions of equal length. It has been checked that this number of regions provides a sufficiently accurate approximation of the functions in the intensity handlers. Notice, however, that the accuracy of this approximation can be improved by setting a higher number of regions. This would imply a higher computational burden to analyse the system. Conversely, the computational load can be reduced by setting less regions, however, this can involve less accurate results.

The units of the variables of the FN in Fig. 12 can be found in Table 4. For the sake of brevity, the reaction fluxes, which are expressed in concentration of the reactant or product per hour, are not reported in the Table. All the values of the parameters used together with their units can be found in Table 5.

The analyses presented in the previous sections focused on the transient behaviour of the systems and obtained

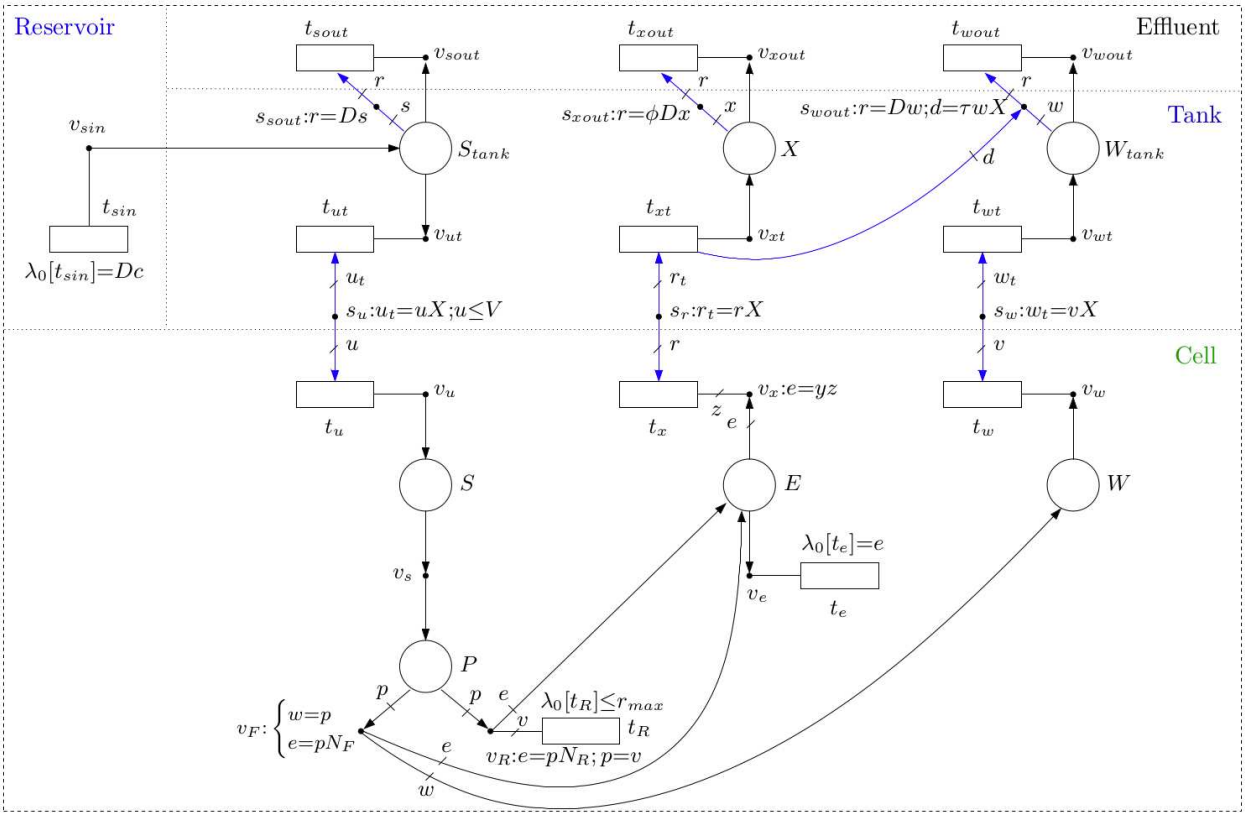

Fig. 12. FN integrating a metabolic network (*Cell* compartment) with the bioreactor dynamics (*Reservoir*, *Tank* and *Effluent* compartments) in continuous culture mode.

Variable	Units	Description
X	$gDW\ L^{-1}$	Cell density
S_{tank}	mM	Nutrient in the tank
W_{tank}	mM	Waste product in the tank
S	$mmol\ gDW^{-1}$	Nutrient in the cells
P	$mmol\ gDW^{-1}$	Intermediate product in the cells
E	$mmol\ gDW^{-1}$	Energetic currency in the cells
W	$mmol\ gDW^{-1}$	Waste product in the cells

Table 4
Units of the variables of the FN in Fig. 12.

time trajectories of the concentration variables. The analysis possibilities of FNs are now exploited to compute the value of the variables at steady state. In [20] mathematical inequalities were derived that account for all the potential steady states that satisfy the constraints defined in the FN. The set of potential states is larger if the constraints are loose, this allows the modeller to check the system possibilities even with highly uncertain parameters at the price of risking the accuracy of the results, the set is smaller if the the constraints are tight. This allows the achievement of accurate results at the price or requiring precise parameters. If there is no uncertainty, then, the system evolves in a deterministic way.

In order to show how uncertain parameters can be handled by FNs, we will assume that the toxicity of the waste product is uncertain, but known to be in the interval $[(1-\epsilon)\tau, (1+\epsilon)\tau]$ where $\tau = 0.0022\ h^{-1}mM^{-1}$ and $\epsilon > 0$ represents the uncertainty of the parameter, e.g. if $\epsilon = 0$ there is no uncertainty. We will assume an uncertainty of 10%, i.e. $\epsilon = 0.1$. This way, the equality d=τwX associated with s_{wout} will be replaced by the inequalities $(1-\epsilon)\tau wX \leq d \leq (1+\epsilon)\tau wX$ in the following.

The FN in Fig. 12 models a nondeterministic system, i.e. different time evolutions and different steady states of the system are consistent with the defined constraints. This nondeterminism derives, not only from the introduced uncertain toxicity of the waste product, but also from the defined flux bounds, e.g. $\lambda_0[t_R]$≤r_{max}, which do not establish a fixed flux, and from the flux fork at some places, e.g. P has two output fluxes which are unrelated

Parameter	Value	Units	Description
D	0.6/24.0	h^{-1}	Dilution rate
c	15	mM	Nutrient concentration in medium
ϕ	0.7	unitless	Bleeding coefficient
N_F	2	unitless	Units of E produced per unit of P
N_R	38	unitless	Units of E produced per unit of P
e	1.0625	$mmol\ gDW^{-1}\ h^{-1}$	Energetic maintenance demand
r_{max}	0.45	$mmol\ gDW^{-1}\ h^{-1}$	Maximum respiratory capacity
V	0.5	$mmol\ gDW^{-1}\ h^{-1}$	Maximum uptake rate of nutrient
y	348	$mmol\ gDW^{-1}$	Energy units needed per unit of biomass produced
τ	0.0022	$h^{-1}mM^{-1}$	Toxicity of waste product

Table 5
Parameters of the FN in Fig. 12.

(different state evolutions will result from the different ways in which these two fluxes can consume P). In order to obtain a particular steady state, an objective function must be added to the set of inequalities obtained in [20]. In a similar way to FBA, the solution of the resulting programming problem yields a steady state that is a theoretical maximum (or minimum depending on the optimization sense) of the objective function. The objective function considered here is the maximization of the cell density, X, which is assumed to be the general tendency of unicells.

3.3 System analysis

Figure 13(a) shows the steady state cell densities, X, obtained by the described programming problem for dilution rates in the interval $[0.01, 2.5]$ day^{-1}, i.e. these cells densities are theoretical maxima for the different dilution rates. The cell density exhibits a rapid increase for low dilution rates and then this increase slows down due to the large amounts of nutrient in the medium required by high cell densities achieved by the retention device. The considered programming problem does not only yield a value for its objective function, but also for all the variables that compose the state of the FN; e.g. concentrations, fluxes, time ratio spent at the different regions, values assigned to the uncertain parameters, etc. Figure 13(b) presents the steady state concentration of the nutrient in the tank. For dilution rates in the range $[0.01, 1.6]$ day^{-1} this concentration is equal to 0, which implies that all the nutrient fed by medium is consumed by the cells. At a dilution rate of 1.6 day^{-1} there is a sudden drop in the cell density, i.e. the FN predicts a dilution washout of 1.6 day^{-1}. The reason for this is that the cell growth and division cannot keep pace with the ever increasing dilution rates. In particular, in this FN this is accounted for by the upper flux bound $\lambda_0[t_R] \leq r_{max}$ imposed on transition t_R. This transition is associated with cellular respiration and its upper bound models the fact that the respiration capacity of the cell is limited. It should be noticed that t_R is the main provider of energy which, in this model, is linked to the growth rate. Thus a limited flux of t_R implies a limited growth rate and, given that the growth rate μ must equal ϕD at steady state (see Eq (1)), a washout takes place for higher values of D. For values of D above the critical dilution rate (which approximates the maximum specific growth rate, μ_{max}), the nutrient starts to accumulate in the tank as it cannot be consumed by the cells at the rate imposed by the applied dilution rate. These plots reproduce the existing dependence of the bioreactor variables with respect to the dilution rate in a continuous culture [23,31,32].

Figures 13(c) and (d) show the steady state fluxes through arcs (P, v_F) and (P, v_R) respectively. Given that the objective function is the maximization of the cell density, the nutrients consumed by the cell have to be used as efficiently as possible to produce energy and, in turn, growth. Since respiration is more efficient for energy production than fermentation ($N_R > N_F$), the solution of the described programming problem diverts as much nutrient as possible towards respiration. This implies that, for low dilution rates, all the nutrient is diverted towards respiration. Thus, the flux through (P, v_R) depends linearly on the dilution rate and the flux through (P, v_F) is 0. At a dilution rate of 1.6 day^{-1}, the flux through (P, v_R) hits the bound $\lambda_0[t_R] \leq r_{max}$. This means that respiration gets saturated and cannot process all the intermediate product for dilution rates higher than 1.6 day^{-1} and, hence, fermentation occurs.

Figures 13(e) and (f) explore the potential concentrations of waste product W in the tank, i.e. they show the minimum and maximum concentrations of W that are compatible with the computed cell densities. In a similar fashion to Flux Variability Analysis [33], the minimum(maximum) W has been computed by a programming problem that fixes the cell density to its maximum value, which has been computed previously, and minimizes(maximizes) the variable W. The maximum value of W represents the highest concentration of toxic waste with which the system can cope whilst still maintaining the cell density for that dilution rate in that particular growth medium.

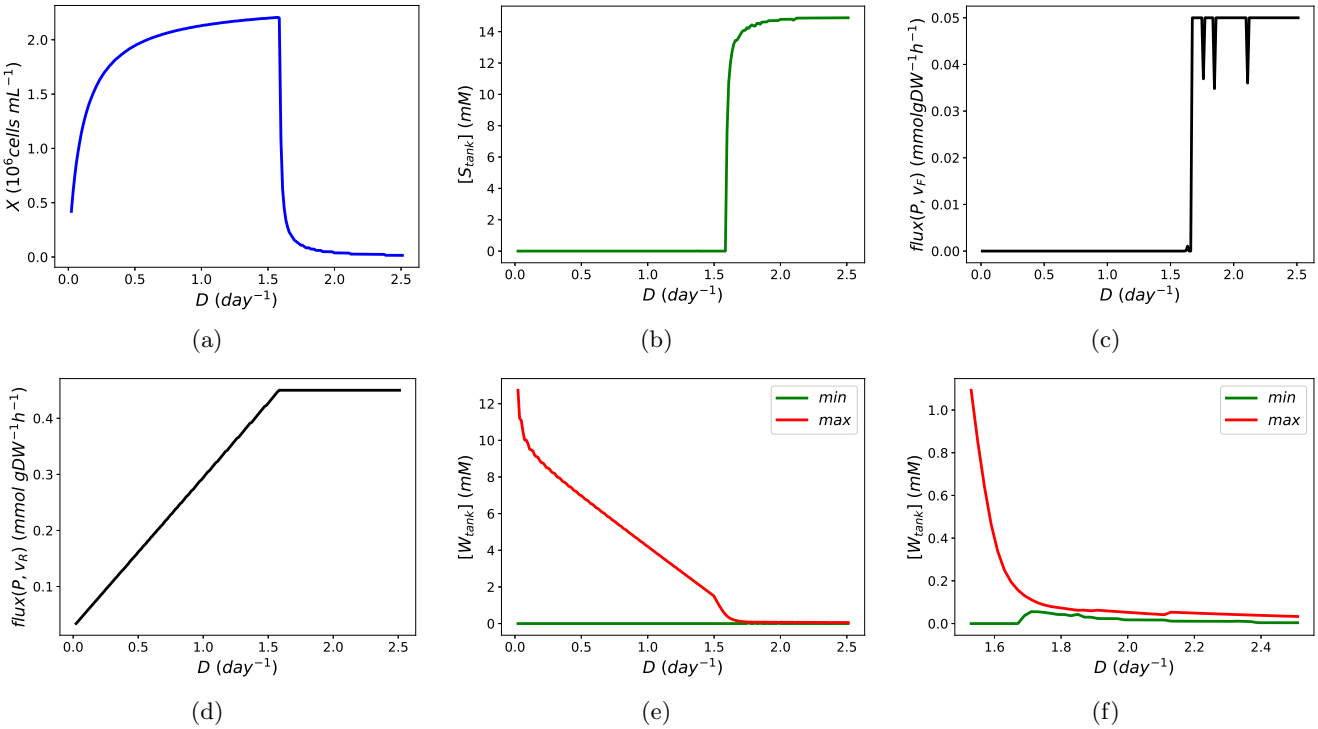

Fig. 13. Steady state variables of the bioreactor and the metabolic network modelled by the FN in Fig. 12 as a function of the dilution rate D: (a) cell density; (b) nutrient concentration in the tank; (c) flux through arc (P, v_F); (d) flux through arc (P, v_R); (e) and (f) minimum and maximum waste product concentration in the tank for different intervals of D.

The minimum values computed for W represent the minimum concentration of waste product that will be found in the tank. For low dilution rates, this minimum concentration is 0, i.e. there might not be toxic product at all. For higher dilution rates (see Fig. 13(f) which zooms out an interval of D) the minimum W becomes strictly positive, which means there will be toxic product in the tank. This is due to a flux of P being diverted to W because reaction R_R is saturated, hence, producing waste product in the tank. Notice that in Fig. 13(f) the values of the minimum and maximum W get rather close. This means that W has not much freedom and, hence, its value is estimated quite accurately.

All the reported results have been computed by the Pyton tool *fnyzer* [19] on an Intel i7 (2.00 GHz, 8 GiB) running Ubuntu 14.04 LTS. The CPU time required to solve the programming problem associated with each dilution rate was 35.78 s.

4 Discussion

Flexible Nets (FNs) is a modelling formalism for dynamic systems inspired by Petri nets that is able to integrate, in a single model, heterogeneous data from different sources. We have shown the potential of FNs to combine stoichiometric models (which lack detailed kinetic information and are mainly expressed as constraint-based models) with kinetic models (which are expressed as differential equations). In addition to subsuming constraint-based models and differential equations, FNs can also accommodate with ease uncertain, i.e. partially known, parameters (both stoichiometric and kinetic). This feature is useful, not only to incorporate imprecise data in the model, but also to estimate the parameter values that are consistent with a given observation of the system.

FNs can be expressed graphically by means of two nets: an event net and an intensity net. While the event net models the system stoichiometry, the intensity net models the system dynamics. Such a graphical representation provides a precise and unambiguous view of the whole system. In addition to its graphical representation, FNs can be expressed by state equations that can be analysed by sets of inequalities derived from them. Such sets of inequalities account for all the potential evolutions of the system and can refer both to its transient or steady state behaviour. This way, the analysis capabilities of FNs cover the analysis methods based on FBA (for constraint-based models) and the analysis methods based on differential equations (for dynamic models), plus offering the facility of coping with uncertain parameters.

In order to obtain a time trajectory of the system, or a steady state value, the mentioned sets of inequalities are associated with an objective function that contains the expression to be optimized. The solution of the resulting programming problem represents a theoretical bound (a maximum, if the objective function is maximized, and

a minimum, if it is minimized) of the optimized expression. If the theoretical minimum and maximum values are close, then the considered expression is estimated accurately, otherwise the expression in the objective function admits a wide range of values, e.g. tolerance to the toxic product in the discussed example in Fig. 12, that are consistent with the model constraints.

With respect to steady state analyses, it should be noted that in order to compute steady states it is not necessary to simulate the transient of the system, the steady state values are directly obtained from the constraints associated with the net. Moreover, balance equations are already taken into account by the mathematical inequalities that are derived automatically from the FN. For instance, in Fig. 12, there is no need to make explicit the balance equation $flux(v_s, P) = flux(P, v_F) + flux(P, v_R)$ (where $flux(a, b)$ denotes the steady state flux from a to b) for the concentration of metabolite P. This constraint will be necessarily satisfied because the average marking of P at the steady state is forced to be constant; hence, the sum of its input fluxes must equal the sum of its output fluxes.

The proposed analysis methods rely on the solution of programming problems derived from the FN model. Thus, the efficiency of the methods is given by the computational burden associated with the algorithms used to solve such programming problems. If all the rates of the reactions are linear, then the resulting programming problems contain exclusively real variables with linear and convex quadratic constraints that can be solved efficiently. Thus, FNs can handle efficiently genome-scale metabolic networks whose kinetic information is mainly given by flux bounds and linear dependencies on the concentrations of metabolites. If the rates are not linear, then these nonlinearities must be approximated by piecewise linear functions which result in mixed-integer linear programming problems with real and binary variables. The complexity involved in the solution of these problems depends primarily on the number of binary variables. Interestingly, the trade-off between the computational burden and the accuracy of the results can be tuned by the modeller by selecting the precision of the approximation of nonlinear functions by piecewise linear functions, i.e. by setting the number of regions to be used and hence increasing or diminishing the number of binary variables in the programming problem.

Data, code and materials: The Python files that define the FNs in Fig. 4, 6, 8, 9 and 12 are `ratecon.py`, `inprod.py`, `hillpwlnet.py`, `modint.py` and `HeLanet.py` respectively. These files, together with `HeLanetss.py`, can be used to obtain numerical values and generate the associated plots. The numerical values of the plots in Fig. 13 can be found in `HeLanetss_results.xls`.

Author's contributions: Both authors have conceived the idea and contributed to writing the manuscript.

Competing interests: We declare we have no competing interests.

Funding: This work was supported by the Spanish Ministry of Science, Innovation and Universities [ref. Medrese-RTI2018-098543-B-I00] to JJ, by the Biotechnology & Biological Sciences Research Council (UK) grant no. BB/N02348X/1 to SGO, as part of the IBiotech Program, and by the Industrial Biotechnology Catalyst (Innovate UK, BBSRC, EPSRC) to support the translation, development and commercialisation of innovative Industrial Biotechnology processes.

References

[1] Machado D, Costa R, Rocha M, Ferreira E, Tidor B, Rocha I. Modeling formalisms in Systems Biology. AMB Express. 2011;1(45):1–14. doi:10.1186/2191-0855-1-45.

[2] Kauffman SA. Metabolic stability and epigenesis in randomly constructed genetic nets. Journal of Theoretical Biology. 1969;22(3):437 – 467. doi:10.1016/0022-5193(69)90015-0.

[3] Wang RS, Saadatpour A, Albert R. Boolean modeling in systems biology: an overview of methodology and applications. Physical Biology. 2012;9(5):055001. doi:10.1088/1478-3975/9/5/055001.

[4] Gupta S, Bisht SS, Kukreti R, Jain S, Brahmachari SK. Boolean network analysis of a neurotransmitter signaling pathway. Journal of Theoretical Biology. 2007;244(3):463 – 469. doi:https://doi.org/10.1016/j.jtbi.2006.08.014.

[5] Needham CJ, Bradford JR, Bulpitt AJ, Westhead DR. A Primer on Learning in Bayesian Networks for Computational Biology. PLOS Computational Biology. 2007 08;3(8):1–8. doi:10.1371/journal.pcbi.0030129.

[6] Grzegorczyk M, Husmeier D, Edwards KD, Ghazal P, Millar AJ. Modelling non-stationary gene regulatory processes with a non-homogeneous Bayesian network and the allocation sampler. Bioinformatics. 2008;24(18):2071–2078. doi:10.1093/bioinformatics/btn367.

[7] Friedman N. Inferring Cellular Networks Using Probabilistic Graphical Models. Science. 2004;303(5659):799–805. doi:10.1126/science.1094068.

[8] Sachs K, Gifford D, Jaakkola T, Sorger P, Lauffenburger DA. Bayesian Network Approach to Cell Signaling Pathway Modeling. Science Signaling. 2002;2002(148):pe38–pe38. doi:10.1126/stke.2002.148.pe38.

[9] Murata T. Petri Nets: Properties, Analysis and Applications. Procs of the IEEE. 1989;77(4):541–580.

[10] Voss K, Heiner M, Koch I. Steady state analysis of metabolic pathways using Petri nets. In silico biology. 2003 02;3:367–87.

[11] Küffner R, Zimmer R, Lengauer T. Pathway analysis in metabolic databases via differential metabolic display (DMD). Bioinformatics. 2000 09;16(9):825–836. doi:10.1093/bioinformatics/16.9.825.

[12] Varma A, Palsson BØ. Metabolic Flux Balancing: Basic Concepts, Scientific and Practical Use. Nature Biotechnology. 1994 Oct;12(10):994–998.

[13] Orth JD, Conrad TM, Na J, Lerman JA, Nam H, Feist AM, et al. A comprehensive genome-scale reconstruction of Escherichia coli metabolism–2011. Molecular Systems Biology. 2011;7(1). doi:10.1038/msb.2011.65.

[14] Tyson JJ, Baumann WT, Chen C, Verdugo A, Tavassoly I, Wang Y, et al. Dynamic modelling of oestrogen signalling and cell fate in breast cancer cells. Nature reviews Cancer. 2011;117:523–32. doi:10.1038/nrc3081.

[15] Millard P, Smallbone K, Mendes P. Metabolic regulation is sufficient for global and robust coordination of glucose uptake, catabolism, energy production and growth in Escherichia coli. PLOS Computational Biology. 2017 02;13(2):1–24. doi:10.1371/journal.pcbi.1005396.

[16] Júlvez J, Dikicioglu D, Oliver SG. Handling variability and incompleteness of biological data by flexible nets: a case study for Wilson disease. npj Systems Biology and Applications. 2018 1;4(1):7. doi:10.1038/s41540-017-0044-x.

[17] Silva M. Introducing Petri Nets. Practice of Petri Nets in Manufacturing. Chapman & Hall, London, 1993;p. 1–62.

[18] Júlvez J, Oliver S. Flexible Nets: a modeling formalism for dynamic systems with uncertain parameters. Discrete Event Dynamic Systems. 2019 08;29:367–392. doi:10.1007/s10626-019-00287-9.

[19] Júlvez J, Oliver SG. *fnyzer* (Flexible Nets analYZER) `https://fnyzer.readthedocs.io`; 2019.

[20] Júlvez J, Oliver SG. Steady State Analysis of Flexible Nets. IEEE Transactions on Automatic Control. 2019;p. 1–1. doi:10.1109/TAC.2019.2931836.

[21] Ben Yahia B, Malphettes L, Heinzle E. Macroscopic modeling of mammalian cell growth and metabolism. Applied Microbiology and Biotechnology. 2015 Sep;99(17):7009–7024. doi:10.1007/s00253-015-6743-6.

[22] Rodríguez-Enríquez S, Marín-Hernández A, Gallardo-Pérez JC, Moreno-Sánchez R. Kinetics of transport and phosphorylation of glucose in cancer cells. Journal of Cellular Physiology. 2009;221(3):552–559. doi:10.1002/jcp.21885.

[23] Fernandez de Cossio Diaz J, Leon K, Mulet R. Characterizing steady states of genome-scale metabolic networks in continuous cell cultures. PLOS Computational Biology. 2017 11;13(11):1–25. doi:10.1371/journal.pcbi.1005835.

[24] Mahadevan R, Edwards JS, Doyle FJ. Dynamic Flux Balance Analysis of Diauxic Growth in Escherichia coli. Biophysical Journal. 2002;83(3):1331 – 1340. doi:https://doi.org/10.1016/S0006-3495(02)73903-9.

[25] Castilho LR, Medronho RA. In: Cell Retention Devices for Suspended-Cell Perfusion Cultures. Berlin, Heidelberg: Springer Berlin Heidelberg; 2002. p. 129–169. doi:10.1007/3-540-45736-4_7.

[26] Pirt SJ. Principles of microbe and cell cultivation. Halsted Press book. Wiley; 1975.

[27] Alberts B, Johnson A, Lewis J, Morgan D, Raff M, Roberts K, et al. Molecular Biology of the Cell. 6th Ed. Garland Science; 2014.

[28] Kilburn DG, Lilly MD, Webb FC. The Energetics of Mammalian Cell Growth. Journal of Cell Science. 1969;4(3):645–654.

[29] Sheikh K, Förster J, Nielsen LK. Modeling Hybridoma Cell Metabolism Using a Generic Genome-Scale Metabolic Model of Mus musculus. Biotechnology Progress. 2005;21(1):112–121. doi:10.1021/bp0498138.

[30] Vazquez A, Liu J, Zhou Y, Oltvai Z. Catabolic efficiency of aerobic glycolysis: The Warburg effect revisited. BMC systems biology. 2010 05;4:58. doi:10.1186/1752-0509-4-58.

[31] Follstad BD, Balcarcel RR, Stephanopoulos G, Wang DIC. Metabolic flux analysis of hybridoma continuous culture steady state multiplicity. Biotechnology and Bioengineering. 1999;63(6):675–683. doi:10.1002/(SICI)1097-0290(19990620)63:6¡675::AID-BIT5¿3.0.CO;2-R.

[32] Konstantinov K, Goudar C, Ng M, Meneses R, Thrift J, Chuppa S, et al. The "Push-to-Low" Approach for Optimization of High-Density Perfusion Cultures of Animal Cells. Advances in biochemical engineering/biotechnology. 2006 02;101:75–98. doi:10.1007/10_016.

[33] Gudmundsson S, Thiele I. Computationally efficient flux variability analysis. BMC bioinformatics. 2010 09;11:489. doi:10.1186/1471-2105-11-489.